Nonlinear Feedback Control of Surface Roughness Using a Stochastic PDE: Design and Application to a Sputtering Process

Yiming Lou[†] **and Panagiotis D. Christofides***[,‡]

Advanced Projects Research, Inc., 1925 McKinley Avenue, Suite B, La Verne, California 91750, and Department of Chemical and Biomolecular Engineering, University of California, Los Angeles, California 90095

In this work, we develop a method for nonlinear feedback control of the roughness of a one-dimensional surface whose evolution is described by the stochastic Kuramoto−Sivashinsky equation (KSE), a fourth-order nonlinear stochastic partial differential equation. We initially formulate the stochastic KSE into a system of infinite nonlinear stochastic ordinary differential equations by using Galerkin's method. A finite-dimensional approximation of the stochastic KSE is then derived that captures the dominant mode contribution to the surface roughness. A nonlinear feedback controller is then designed based on the finite-dimensional approximation to control the surface roughness. An analysis of the closed-loop nonlinear infinite-dimensional system is performed to characterize the closed-loop performance enforced by the nonlinear feedback controller in the closed-loop infinite-dimensional system. The effectiveness of the proposed nonlinear controller and the advantages of the nonlinear controller over a linear controller resulting from the linearization of the nonlinear controller around the zero solution are demonstrated through numerical simulations. Finally, a successful application of a stochastic KSE-based nonlinear feedback controller to the kinetic Monte Carlo model of a sputtering process is also demonstrated.

1. Introduction

The surface roughness of thin films strongly affects the quality of such films and consequently is an important variable to control. Therefore, modeling and control of thin film microstructure have attracted significant research efforts in the recent years. Fundamental mathematical modeling techniques have been developed to describe the microscopic features of surfaces formed by surface microprocesses, which include (1) dynamical Monte Carlo methods[1−4] and (2) stochastic partial differential equations.[5−8] The development of modern roughness measurement techniques provides the opportunity to obtain roughness measurements in real-time using spectroscopic ellipsometry techniques,[9] by grazing-incidence small-angle X-ray scattering (GISAXS),[10] or by combination of on-line measurement techniques for measuring gas-phase compositions with off-line measurement techniques for measuring surface roughness. An implementation of the latter approach was recently reported in ref 11 where it was used to measure carbon composition of thin films in plasma-enhanced chemical vapor deposition using combination of optical emission spectroscopy (OES) and X-ray photoelectron spectroscopy (XPS). Also, experimental methods have been developed to perform scanning tunneling microscopy (STM) measurement on the surface during epitaxial growth of semiconductor layers.[12]

The kinetic Monte Carlo simulation methods can be used to predict average properties of thin films (which are of interest from a control point of view, for example, surface roughness), by explicitly accounting for the microprocesses that directly shape thin film microstructure. A methodology for feedback control of surface roughness using kinetic Monte Carlo models was developed in refs 13 and 14. The methodology led to the design of (a) real-time roughness estimators by using multiple small lattice kinetic Monte Carlo simulators, adaptive filters, and measurement error compensators and (b) feedback controllers based on the real-time roughness estimators. The method was successfully applied to control surface roughness in a GaAs deposition process model.[15] Moreover, kinetic Monte Carlo methods were also used to study dynamics of complex deposition processes including multiple components with both short-range and long-range interactions and to perform predictive control design to control final surface roughness in ref 16.

However, the fact that kinetic Monte Carlo models are not available in closed-form makes it very difficult to use them for system-level analysis and the design and implementation of model-based feedback control systems. To achieve better closed-loop performance, it is desirable to design feedback controllers on the basis of deposition process models. An approach was reported in refs 17 and 18 to identify linear deterministic models from outputs of kinetic Monte Carlo simulators and design controllers using linear control theory. This approach is effective in controlling macroscopic variables, which are low statistical moments of the microscopic distributions (e.g., surface coverage, which is the zeroth moment of species distribution on a lattice). However, to control higher statistical moments of the microscopic distributions, such as the surface roughness (the second moment of height distribution on a lattice) or even the microscopic configuration (such as the surface morphology), deterministic models may not be sufficient. This is because the effect of the stochastic nature of the microscopic processes becomes very significant in these cases and must be addressed in both the model construction and controller design. On the other hand, stochastic PDEs contain the surface morphology information of thin films; thus, they may be used for the purpose of feedback controller design. For example, it has been experimentally verified that the Kardar−Parisi−Zhang (KPZ) equation[19] can describe the evolution of the surface morphology of gallium arsenide (GaAs) thin films, which is consistent with the surface measured by atomic force microscopy (AFM).[20,21] Furthermore, based on the fact that kinetic Monte Carlo

* Corresponding author. Tel: (310)794-1015. Fax: (310)206-4107. E-mail: pdc@seas.ucla.edu.

[†] Advanced Projects Research, Inc.

[‡] University of California, Los Angeles.

10.1021/ie060410h CCC: $33.50
Published on Web 09/13/2006

simulations provide realizations of a stochastic process that are consistent with the master equation that describes the evolution of the probability distribution of the system being at a certain microconfiguration, a method to construct reduced-order approximations of the master equation was reported in ref 22. Recently, a method was also developed to identify an empirical input−output model for a copper electrodeposition process using simulation data from a coupled kinetic Monte Carlo and finite-difference simulation code and perform controller design using the identified model.[23]

For many deposition and sputtering processes, closed-form process models, in the form of linear or nonlinear stochastic partial differential equations (PDEs), can be derived based on the microscopic rules and the corresponding master equation (e.g., refs 5−8 and 24). To achieve better closed-loop performance, it is desirable to design feedback controllers on the basis of process models. This has motivated recent research on the development of a method for feedback control of surface roughness based on linear stochastic PDE process models.[25,26] This method involves reformulation of the linear stochastic PDE into a system of infinite linear stochastic ordinary differential equations (ODEs) by using modal decomposition, derivation of a finite-dimensional approximation that captures the dominant mode contribution to the surface roughness, and state feedback controller design based on the finite-dimensional approximation. Furthermore, a method for construction of linear stochastic PDE models for thin film growth using first principles-based microscopic simulations was developed in ref 27, and a multi-variable predictive control based on a linear stochastic PDE model was developed in ref 28 to simultaneously control surface roughness and growth rate in a thin film deposition process taking place in a 2-D lattice.

However, nonlinearities exist in many material preparation processes in which surface evolution can be modeled by stochastic PDEs. A typical example of such processes is the sputtering process whose surface evolution is described by the nonlinear stochastic Kuramoto−Sivashinsky equation (KSE). In a simplified setting, the sputtering process includes two types of surface microprocesses, erosion and diffusion. The nonlinearity of the sputtering process originates from the dependence of the rate of erosion on a nonlinear sputtering yield function.[7] In our previous work,[26] feedback control of surface roughness in sputtering processes was designed based on a linearized stochastic KSE process model, which was identified by using data from multiple kinetic Monte Carlo simulations of the same process. However, it is expected that such a linear controller is only going to provide good closed-loop performance locally (i.e., for initial conditions close to the desired set point) for the nonlinear closed-loop system, due to the fact that the inherent process nonlinearities are not explicitly considered in the linearized process model. To perform feedback control design for nonlinear stochastic processes (i.e., provide good performance for a wide range of process initial conditions and operating conditions), it is desirable that a nonlinear process model is directly used as the basis for controller synthesis. This motivates research on nonlinear feedback control of nonlinear stochastic PDEs.

In this work, we develop a method for nonlinear feedback control of the roughness of a one-dimensional surface whose evolution is described by the stochastic KSE. A finite-dimensional approximation of the stochastic KSE is first derived that captures the dominant mode contribution to the surface roughness and a nonlinear feedback controller is designed based on this finite-dimensional approximation to control the surface roughness. An analysis of the closed-loop nonlinear infinite-dimensional system is performed to characterize the closed-loop performance enforced by the nonlinear feedback controller in the closed-loop infinite-dimensional system. The proposed nonlinear controller is successfully applied to a high-order approximation of the stochastic KSE and the kinetic Monte Carlo model of a sputtering process.

2. Preliminaries

The stochastic KSE is a fourth-order nonlinear stochastic partial differential equation that describes the evolution of the height fluctuation for surfaces in a variety of material preparation processes including surface erosion by ion sputtering,[7,8] surface smoothing by energetic clusters,[29] and ZrO_2 thin film growth by reactive ion beam sputtering.[30] We consider the stochastic KSE in a one-dimensional domain[8] with distributed control in the spatial domain $[-\pi, \pi]$ (see also refs 31−34 for distributed control problem formulation for the deterministic KSE):

$$\frac{\partial h}{\partial t} = -\nu\frac{\partial^2 h}{\partial x^2} - \kappa\frac{\partial^4 h}{\partial x^4} + \frac{\lambda}{2}\left(\frac{\partial h}{\partial x}\right)^2 + \sum_{i=1}^{p} b_i(x)u_i(t) + \xi(x, t) \quad (1)$$

subject to periodic boundary conditions:

$$\frac{\partial^j h}{\partial x^j}(-\pi, t) = \frac{\partial^j h}{\partial x^j}(\pi, t) \quad j = 0, ..., 3 \quad (2)$$

and the initial condition:

$$h(x, 0) = h_0(x) \quad (3)$$

where ν, κ, and λ are parameters related to surface mechanisms,[30] $x \in [-\pi, \pi]$ is the spatial coordinate, t is the time, $h(x, t)$ is the height of the surface at position x and time t, u_i is the ith manipulated input, p is the number of manipulated inputs, and b_i is the ith actuator distribution function (i.e., b_i determines how the control action computed by the ith control actuator, u_i, is distributed (e.g., point or distributed actuation) in the spatial interval $[-\pi, \pi]$). $\xi(x, t)$ is a Gaussian noise with the following expressions for its mean and covariance:

$$\langle \xi(x, t) \rangle = 0$$
$$\langle \xi(x, t)\xi(x', t') \rangle = \delta(x - x')\delta(t - t') \quad (4)$$

where $\delta(\cdot)$ is the dirac function and $\langle \cdot \rangle$ denotes the expected value. Note that the noise covariance depends on both space x and time t.

Our objective is to control the expected roughness of the surface described by the stochastic KSE. The surface roughness, r, is represented by the standard deviation of the surface from its average height and is computed as follows:

$$r(t) = \sqrt{\frac{1}{2\pi}\int_{-\pi}^{\pi} [h(x, t) - \bar{h}(t)]^2 \, dx} \quad (5)$$

where

$$\bar{h}(t) = \frac{1}{2\pi}\int_{-\pi}^{\pi} h(x, t) \, dx$$

is the average surface height.

To study the dynamics of eq 1, we initially consider the eigenvalue problem of the linear operator of eq 1, which takes the form:

$$A\bar{\phi}_n(x) = -\nu\frac{d^2\bar{\phi}_n(x)}{dx^2} - \kappa\frac{d^4\bar{\phi}_n(x)}{dx^4} = \lambda_n\bar{\phi}_n(x)$$

$$\frac{d^j\bar{\phi}_n}{dx^j}(-\pi) = \frac{d^j\bar{\phi}_n}{dx^j}(+\pi) \quad j = 0, ..., 3; \quad n = 1, ..., \infty \quad (6)$$

where λ_n denotes an eigenvalue and $\bar{\phi}_n$ denotes an eigenfunction. A direct computation of the solution of the above eigenvalue problem yields $\lambda_0 = 0$ with $\psi_0 = 1/\sqrt{2\pi}$, and $\lambda_n = \nu n^2 - \kappa n^4$ (λ_n is an eigenvalue of multiplicity two) with eigenfunctions $\phi_n = (1/\sqrt{\pi})\sin(nx)$ and $\psi_n = (1/\sqrt{\pi})\cos(nx)$ for $n = 1, ..., \infty$. Note that the $\bar{\phi}_n$ in eq 6 denotes either ϕ_n or ψ_n. From the expression of the eigenvalues, it follows that for fixed values of $\nu > 0$ and $\kappa > 0$, the number of unstable eigenvalues of the operator A in eq 6 is finite and the distance between two consecutive eigenvalues (i.e. λ_n and λ_{n+1}) increases as n increases.

To present the method that we use to control eq 1, we first derive nonlinear stochastic ODE approximations of eq 1 using Galerkin's method. To this end, we first expand the solution of eq 1 in an infinite series in terms of the eigenfunctions of the operator of eq 6 as follows:

$$h(x, t) = \sum_{n=1}^{\infty}\alpha_n(t)\phi_n(x) + \sum_{n=0}^{\infty}\beta_n(t)\psi_n(x) \quad (7)$$

where $\alpha_n(t)$ and $\beta_n(t)$ are time-varying coefficients. Substituting the above expansion for the solution, $h(x, t)$, into eq 1 and taking the inner product with the adjoint eigenfunctions, $\phi_n^*(z) = (1/\sqrt{\pi})\sin(nz)$ and $\psi_n^*(z) = (1/\sqrt{\pi})\cos(nz)$, the following system of infinite nonlinear stochastic ODEs is obtained:

$$\frac{d\alpha_n}{dt} = (\nu n^2 - \kappa n^4)\alpha_n + f_{n\alpha} + \sum_{i=1}^{p} b_{i\alpha_n}u_i(t) + \xi_\alpha{}^n(t) \quad n = 1, ..., \infty$$

$$\frac{d\beta_n}{dt} = (\nu n^2 - \kappa n^4)\beta_n + f_{n\beta} + \sum_{i=1}^{p} b_{i\beta_n}u_i(t) + \xi_\beta{}^n(t) \quad (8)$$

where

$$f_{n\alpha} = \frac{\lambda}{2}\int_{-\pi}^{\pi}\phi_n(x)\left(\sum_{j=1}^{\infty}\alpha_j(t)\frac{d\phi_j}{dx}(x) + \sum_{j=0}^{\infty}\beta_j(t)\frac{d\psi_j}{dx}(x)\right)^2 dx$$

$$f_{n\beta} = \frac{\lambda}{2}\int_{-\pi}^{\pi}\psi_n(x)\left(\sum_{j=1}^{\infty}\alpha_j(t)\frac{d\phi_j}{dx}(x) + \sum_{j=0}^{\infty}\beta_j(t)\frac{d\psi_j}{dx}(x)\right)^2 dx \quad (9)$$

and

$$b_{i\alpha_n} = \int_{-\pi}^{\pi}\phi_n(x)b_i(x)\,dx$$

$$b_{i\beta_n} = \int_{-\pi}^{\pi}\psi_n(x)b_i(x)\,dx$$

$$\xi_\alpha{}^n(t) = \int_{-\pi}^{\pi}\xi(x, t)\phi_n(x)\,dx$$

$$\xi_\beta{}^n(t) = \int_{-\pi}^{\pi}\xi(x, t)\psi_n(x)\,dx \quad (10)$$

The covariances of $\xi_\alpha{}^n(t)$ and $\xi_\beta{}^n(t)$ can be computed by using the following result:

Result 1. If (1) $f(x)$ is a deterministic function, (2) $\eta(x)$ is a random process with $\langle\eta(x)\rangle = 0$ and covariance $\langle\eta(x)\eta(x')\rangle = \sigma^2\delta(x - x')$, and (3) $\epsilon = \int_a^b f(x)\eta(x)\,dx$, then ϵ is a random number with $\langle\epsilon\rangle = 0$ and covariance $\langle\epsilon^2\rangle = \sigma^2\int_a^b f^2(x)\,dx$.[35]

Using Result 1, we obtain $\langle\xi_\alpha{}^n(t)\xi_\alpha{}^n(t')\rangle = \delta(t - t')$ and $\langle\xi_\beta{}^n(t)\xi_\beta{}^n(t')\rangle = \delta(t - t')$.

In this work, the controlled variable is the expected value of the square of the surface roughness defined in eq 5, $\langle r(t)^2\rangle$. According to eq 7, we have $\bar{h}(t) = \beta_0(t)\psi_0$. Therefore, $\langle r(t)^2\rangle$ can be rewritten in terms of $\alpha_n(t)$ and $\beta_n(t)$ as follows:

$$\langle r(t)^2\rangle = \frac{1}{2\pi}\left\langle\int_{-\pi}^{\pi}(h(x, t) - \bar{h}(t))^2\,dx\right\rangle$$

$$= \frac{1}{2\pi}\left\langle\int_{-\pi}^{\pi}\left[\sum_{i=1}^{\infty}\alpha_i(t)\phi_i(x) + \sum_{i=0}^{\infty}\beta_i(t)\psi_i(x) - \beta_0(t)\psi_0\right]^2 dx\right\rangle$$

$$= \frac{1}{2\pi}\left\langle\int_{-\pi}^{\pi}\sum_{i=1}^{\infty}[\alpha_i(t)^2\phi_i(x)^2 + \beta_i(t)^2\psi_i(x)^2]\,dx\right\rangle$$

$$= \frac{1}{2\pi}\left\langle\sum_{i=1}^{\infty}(\alpha_i(t)^2 + \beta_i(t)^2)\right\rangle = \frac{1}{2\pi}\sum_{i=1}^{\infty}[\langle\alpha_i(t)^2\rangle + \langle\beta_i(t)^2\rangle] \quad (11)$$

Therefore, the surface roughness control problem for the stochastic KSE of eq 1 is formulated as the one of controlling the covariance of the states α_n and β_n in the nonlinear stochastic ODE system of eq 8.

Remark 1. Note that in practice, the control action, u_i, can be implemented by manipulating the gas composition across the surface in either a deposition process or a sputtering process. Spatially controllable CVD reactors have been developed to enable across-wafer spatial control of surface gas composition during deposition.[36] In such a control problem formulation, the rate that particles land on the surface or the rate that surface particles are eroded is spatially distributed and is computed by the controller. The parameters of the stochastic KSE model of eq 1 depend on both the temperature and the rate that particles land on the surface or that surface particles are eroded.[8] In this work, the temperature is assumed to be a constant. The rate that particles land on the surface or the rate that surface particles are eroded used to compute the stochastic KSE model parameters corresponds to that under open-loop operation, and thus, it is also a constant. The contribution of the spatially distributed rate that particles land on the surface or the rate that surface particles are eroded to the fluctuations of the surface height profile (e.g., the surface roughness) is captured by the term $\sum_{i=1}^{p} b_i(x)u_i(t)$. This control problem formulation is further supported by our simulation results, which demonstrate that the controller designed on the basis of the stochastic KSE model of a sputtering process can be successfully applied to the kinetic Monte Carlo model of the same sputtering process to control the surface roughness to desired levels (see simulation results section).

Remark 2. Note that in the stochastic KSE of eq 1, the covariance of $\xi(x, t)$ is normalized to be $\delta(x - x')\delta(t - t')$. In general, the covariance of the noise term of the stochastic KSE is $\varsigma^2\delta(x - x')\delta(t - t')$, where ς^2 is a process parameter derived based on the rates of surface microscopic processes.[7] The normalization procedure is detailed in the simulation section of this work. This convenience is adopted to simplify our presentation.

Remark 3. Note that because the term β_0 is canceled in the computation of the expected value of the surface roughness, defined in eq 11, β_0 does not contribute to the expected surface roughness. Therefore, the stochastic ODE related to β_0 in the system of eq 8 is not considered in the development of the feedback controller for surface roughness control in the next section.

Remark 4. Stochastic PDE models for many deposition processes and sputtering processes can be derived based on the corresponding master equations, which describe the evolution of the probability that the surface is at a certain configuration (see, for example, refs 8 and 37). The surface in these processes is directly formed by microscopic events such as adsorption, desorption, erosion, diffusion, and reaction. Kinetic Monte Carlo simulation can also be used to predict the evolution of the surface configuration in stochastic processes. The kinetic Monte Carlo model is a first-principle model in the sense that the microscopic rules are explicitly considered in the model. Mathematically, kinetic Monte Carlo simulation methods provide an unbiased realization of the master equation. Therefore, the evolution of the surface configuration predicted by the closed-form stochastic PDE model is consistent with that predicted by the kinetic Monte Carlo model. As a result, the controller designed based on the stochastic PDE process model can be applied to the kinetic Monte Carlo model of the same process.[25,26] In the simulation section, we will demonstrate nonlinear control of a sputtering process including two surface microprocesses, diffusion and erosion. The fluctuation of surface height of such a sputtering process can be described by the stochastic KSE. A nonlinear feedback controller will be designed based on the stochastic KSE process model and will be applied to the kinetic Monte Carlo model of the same process to control the surface roughness to a desired level.

Remark 5. It is also important to note that the problem of feedback control of the deterministic KSE, which is used to describe incipient instabilities in a variety of physical/chemical processes including falling liquid films, unstable flame fronts, and interfacial instabilities between two viscous fluids, has attracted significant research effort. Analytical and numerical studies of the dynamics of the deterministic KSE have revealed that the dominant dynamics of the KSE can be adequately characterized by a small number of degrees of freedom.[38] This has motivated extensive research focusing on the design of linear/nonlinear finite-dimensional output feedback controllers[31,32] for stabilization of the zero solution of the KSE on the basis of ordinary differential equation approximations, obtained through linear[32] and nonlinear[31] Galerkin's method, that accurately describe the dominant dynamics of the KSE for a given value of the instability parameter. The accuracy of the solutions of the ODE systems obtained through Galerkin's method to the ones of the PDE can be analyzed by using a methodology developed in.[39] The global stabilization of the KSE has also been addressed via distributed static output feedback control.[33] A nonlinear boundary feedback controller was also proposed in ref 40 that enhances the rate of convergence to the spatially uniform steady state of the KSE, for values of the instability parameter for which this steady state is open-loop stable. The issue of optimal actuator/sensor placement for the KSE was also addressed in ref 34 so that the desired control objectives are achieved with minimal energy use.

3. Feedback Control

In this section, we design a nonlinear state feedback controller for the system of eq 8 so that the expected value of the surface roughness defined in eq 11 can be controlled to a desired level.

3.1. Model Reduction. Owing to its infinite-dimensional nature, the system of eq 8 cannot be directly used for the design of controllers that can be implemented in practice (i.e., the practical implementation of controllers that are designed on the basis of this system will require the computation of infinite sums which cannot be done by a computer). Instead, we will base the controller design on a finite-dimensional approximation of this system. Subsequently, we will show that the resulting controller will enforce the desired control objective in the closed-loop infinite-dimensional system. Specifically, we rewrite the system of eq 8 as follows:

$$\frac{dx_s}{dt} = \Lambda_s x_s + f_s(x_s, x_f) + B_s u + \xi_s$$

$$\frac{dx_f}{dt} = \Lambda_f x_f + f_f(x_s, x_f) + B_f u + \xi_f \tag{12}$$

where $x_s = [\alpha_1 \cdots \alpha_m\ \beta_1 \cdots \beta_m]^T$, $x_f = [\alpha_{m+1}\ \beta_{m+1} \cdots]^T$, $\Lambda_s = \mathrm{diag}[\lambda_1 \cdots \lambda_m\ \lambda_1 \cdots \lambda_m]$, $\Lambda_f = \mathrm{diag}[\lambda_{m+1}\ \lambda_{m+1}\ \lambda_{m+2}\ \lambda_{m+2} \cdots]$, $f_s(x_s, x_f) = [f_{1\alpha}(x_s, x_f) \cdots f_{m\alpha}(x_s, x_f)\ f_{1\beta}(x_s, x_f) \cdots f_{m\beta}(x_s, x_f)]^T$, $f_f(x_s, x_f) = [f_{m+1\alpha}(x_s, x_f)\ f_{m+1\beta}(x_s, x_f) \cdots]^T$, $u = [u_1 \cdots u_p]$, $\xi_s = [\xi_\alpha{}^1 \cdots \xi_\alpha{}^m\ \xi_\beta{}^1 \cdots \xi_\beta{}^m]$, and $\xi_f = [\xi_\alpha{}^{m+1}\ \xi_\beta{}^{m+1} \cdots]$:

$$B_s = \begin{bmatrix} b_{1\alpha_1} & \cdots & b_{p\alpha_1} \\ \vdots & \ddots & \vdots \\ b_{1\alpha_m} & \cdots & b_{p\alpha_m} \\ b_{1\beta_1} & \cdots & b_{p\beta_1} \\ \cdots & \ddots & \vdots \\ b_{1\beta_m} & \cdots & b_{p\beta_m} \end{bmatrix}$$

$$B_f = \begin{bmatrix} b_{1\alpha_{m+1}} & \cdots & b_{p\alpha_{m+1}} \\ b_{1\beta_{m+1}} & \cdots & b_{p\beta_{m+1}} \\ b_{1\alpha_{m+2}} & \cdots & b_{p\alpha_{m+2}} \\ b_{1\beta_{m+2}} & \cdots & b_{p\beta_{m+2}} \\ \vdots & \vdots & \vdots \end{bmatrix} \tag{13}$$

In our development, we will need the following notations. The 2-norms for vectors x_s, x_f, and $f_s(x_s, x_f)$ are defined as follows:

$$||x_s||_2 = \sqrt{\sum_{j=1}^{m} \alpha_j{}^2 + \sum_{j=1}^{m} \beta_j{}^2}$$

$$||x_f||_2 = \sqrt{\sum_{j=m+1}^{\infty} \alpha_j{}^2 + \sum_{j=m+1}^{\infty} \beta_j{}^2}$$

$$||f_s(x_s, x_f)||_2 = \sqrt{\sum_{j=1}^{m} f_{j\alpha}(x_s, x_f)^2 + \sum_{j=1}^{m} f_{j\beta}(x_s, x_f)^2} \tag{14}$$

The covariance matrices for $x_s(t)$ and $x_f(t)$, $P_s(t)$ and $P_f(t)$ are defined as follows:

$$P_s(t) = \langle x_s(t) x_s{}^T(t) \rangle \quad P_f(t) = \langle x_f(t) x_f{}^T(t) \rangle \tag{15}$$

where $\langle \cdot \rangle$ denotes the expected value and $x_s{}^T(t)$ and $x_f{}^T(t)$ are transposes of the vectors $x_s(t)$ and $x_f(t)$, respectively.

We note that the subsystem x_f in eq 12 is infinite-dimensional. Neglecting the x_f subsystem, the following $2m$-dimensional system is obtained:

$$\frac{d\tilde{x}_s}{dt} = \Lambda_s \tilde{x}_s + f_s(\tilde{x}_s, 0) + B_s u + \xi_s \tag{16}$$

where the tilde symbol in $\tilde{x}_s$ denotes that this state variable is associated with a finite-dimensional system.

3.2. Feedback Control Design. We design the nonlinear state feedback controller on the basis of eq 16. To simplify our development, we assume that $p = 2m$ (i.e., the number of control actuators is equal to the dimension of the finite-dimensional system) and pick the actuator distribution functions such that B_s^{-1} exists. The state feedback control law then takes the form:

$$u = B_s^{-1}\{(\Lambda_{cs} - \Lambda_s)\tilde{x}_s - f_s(\tilde{x}_s, 0)\} \tag{17}$$

where the matrix Λ_{cs} contains the desired poles of the closed-loop system; $\Lambda_{cs} = \mathrm{diag}[\lambda_{c\alpha 1} \cdots \lambda_{c\alpha m}\ \lambda_{c\beta 1} \cdots \lambda_{c\beta m}]$, $\lambda_{c\alpha i}$ and $\lambda_{c\beta i}$ $(1 \le i \le m)$ are desired poles of the closed-loop finite-dimensional system, which satisfy $Re\{\lambda_{c\alpha i}\} < 0$ and $Re\{\lambda_{c\beta i}\} < 0$ for $(1 \le i \le m)$ and can be determined from the desired closed-loop surface roughness level. The method to determine the eigenvalues of Λ_{cs} will be discussed in section 3.3.

The control action is computed using the formula of eq 17, and the computation cost is growing with the number of actuators, p. Since B_s^{-1} depends only on the configuration of the control actuators, it can be computed off-line. The major computational requirement involved in eq 17 is the evaluation of the nonlinear term $f_s(\tilde{x}_s, 0)$, whose specific form is given in eq 18 below:

$$f_s(\tilde{x}_s, 0) = [f_{1\alpha}(\tilde{x}_s, 0) \cdots f_{m\alpha}(\tilde{x}_s, 0) f_{1\beta}(\tilde{x}_s, 0) \cdots f_{m\beta}(\tilde{x}_s, 0)]^T$$

$$f_{n\alpha}(\tilde{x}_s, 0) = \frac{\lambda}{2}\int_{-\pi}^{\pi} \phi_n(x)\left(\sum_{j=1}^{m} \alpha_j(t)\frac{d\phi_j}{dx}(x) + \sum_{j=1}^{m} \beta_j(t)\frac{d\psi_j}{dx}(x)\right)^2 dx \qquad n = 1, \ldots, m$$

$$f_{n\beta}(\tilde{x}_s, 0) = \frac{\lambda}{2}\int_{-\pi}^{\pi} \psi_n(x)\left(\sum_{j=1}^{m} \alpha_j(t)\frac{d\phi_j}{dx}(x) + \sum_{j=1}^{m} \beta_j(t)\frac{d\psi_j}{dx}(x)\right)^2 dx \tag{18}$$

Therefore, the computation of $f_s(\tilde{x}_s, 0)$ involves standard numerical operations and can be completed very fast relative to the time scale of process evolution using currently available computing power.

We will show in section 3.3 that the expected surface roughness of the closed-loop infinite-dimensional system of eq 8 can be controlled to the desired level by using the state feedback controller of eq 17, which only uses a finite number of actuators.

3.3. Analysis of the Closed-Loop Infinite-Dimensional System. By applying the controller of eq 17 to the infinite-dimensional system of eq 12, and using that $\epsilon = |\lambda_1|/|\lambda_{m+1}|$, the closed-loop system takes the form:

$$\frac{dx_s}{dt} = \Lambda_{cs} x_s + (f_s(x_s, x_f) - f_s(x_s, 0)) + \xi_s$$

$$\epsilon\frac{dx_f}{dt} = \Lambda_{f\epsilon} x_f + \epsilon B_f B_{s-1}(\Lambda_{cs} - \Lambda_s)\tilde{x}_s + \epsilon f_f(x_s, x_f) - \epsilon B_f B_s^{-1} f_s(\tilde{x}_s, 0) + \epsilon\xi_f \tag{19}$$

where λ_1 and λ_{m+1} are the first and the $(m+1)$th eigenvalues of the linear operator in eq 6, and $\Lambda_{f\epsilon} = \mathrm{diag}[\lambda_{\epsilon 1}\ \lambda_{\epsilon 1}\ \lambda_{\epsilon 2}\ \lambda_{\epsilon 2} \cdots]$ is an infinite-dimensional matrix defined as $\Lambda_{f\epsilon} = \epsilon \cdot \Lambda_f$.

Computing the linearization of the nonlinear system of eq 19 around $(x_s, x_f) = (0, 0)$ and using the fact that the terms $\{f_s(x_s, x_f) - f_s(x_s, 0)\}$, $f_f(x_s, x_f)$, and $f_s(x_s, 0)$ include terms of second-order and do not include linear terms (this follows from the quadratic structure of the nonlinear term of the stochastic KSE and from eq 9), we obtain the following linear system:

$$\frac{dx_s}{dt} = \Lambda_{cs} x_s + \xi_s$$

$$\epsilon\frac{dx_f}{dt} = \Lambda_{f\epsilon} x_f + \epsilon B_f B_s^{-1}(\Lambda_{cs} - \Lambda_s)\tilde{x}_s + \epsilon\xi_f \tag{20}$$

Owing to the stability properties of Λ_{cs} and $\Lambda_{f\epsilon}$ and the decoupled nature of the system of eq 20, this system is asymptotically stable; thus, the nonlinear system of eq 19 is locally (i.e., for sufficiently small initial conditions) asymptotically stable. This implies that under the assumption that the initial condition is sufficient small, as $t \to \infty$, the covariance matrices of x_s and x_f of the system of eq 19 converge to $P_s(\infty)$ and $P_f(\infty)$, respectively. $P_s(\infty)$ and $P_f(\infty)$ are defined as follows:

$$P_s(\infty) = \lim_{t\to\infty} \langle x_s(t) x_s^T(t)\rangle \quad P_f(\infty) = \lim_{t\to\infty} \langle x_f(t) x_f^T(t)\rangle \tag{21}$$

where $\langle\cdot\rangle$ denotes the expected value, and $x_s^T(t)$ and $x_f^T(t)$ are transposes of the vectors $x_s(t)$ and $x_f(t)$, respectively.

We now proceed to characterize the accuracy with which the closed-loop surface roughness is controlled. Theorem 1 provides estimates of the contribution of the expected surface roughness from the x_s and x_f subsystems of the closed-loop system of eq 19 and a characterization of the expected value of the surface roughness enforced by the controller of eq 17 in the closed-loop stochastic KSE. The proof of Theorem 1 is given in the Appendix.

Theorem 1. Consider the closed-loop stochastic KSE of eq 19. Define the expected surface roughness and the contribution to the expected surface roughness of the closed-loop system from the x_f and x_s subsystems as $t \to \infty$ as follows:

$$\langle r(\infty)^2\rangle = \frac{1}{2\pi}\sum_{i=1}^{\infty}[\langle\alpha_i(\infty)^2\rangle + \langle\beta_i(\infty)^2\rangle]$$

$$\langle r_f(\infty)^2\rangle = \frac{1}{2\pi}\sum_{i=m+1}^{\infty}[\langle\alpha_i(\infty)^2\rangle + \langle\beta_i(\infty)^2\rangle]$$

$$\langle r_s(\infty)^2\rangle = \frac{1}{2\pi}\sum_{i=1}^{m}[\langle\alpha_i(\infty)^2\rangle + \langle\beta_i(\infty)^2\rangle] \tag{22}$$

where $\langle\cdot\rangle$ denotes the expected value, $\langle r(\infty)^2\rangle$ is the expected surface roughness of the closed-loop system of eq 19, $\langle r_f(\infty)^2\rangle$ is the contribution to the expected surface roughness from the x_f subsystem of eq 19, $\langle r_s(\infty)^2\rangle$ is the contribution to the expected surface roughness from the x_s subsystem of eq 19, $x_f = [\alpha_{m+1}\ \beta_{m+1}\ \alpha_{m+2}\ \beta_{m+2} \cdots]^T$, and $x_s = [\alpha_1 \cdots \alpha_m\ \beta_1 \cdots \beta_m]^T$.

Then, there exist $\mu^* > 0$ and $\epsilon^* > 0$ such that if $||x_{f0}||_2 + ||x_{s0}||_2 \le \mu^*$ and $\epsilon \in (0, \epsilon^*]$, $\langle r_f(\infty)^2\rangle$, $\langle r_s(\infty)^2\rangle$, and $\langle r(\infty)^2\rangle$ satisfy:

$$\langle r_f(\infty)^2\rangle = O(\epsilon) \tag{23}$$

$$\langle r_s(\infty)^2\rangle = \frac{1}{4\pi}\sum_{i=1}^{m}\left(\frac{1}{|\lambda_{c\alpha i}|} + \frac{1}{|\lambda_{c\beta i}|}\right) + O(\sqrt{\epsilon}) \tag{24}$$

$$\langle r(\infty)^2\rangle = \frac{1}{4\pi}\sum_{i=1}^{m}\left(\frac{1}{|\lambda_{c\alpha i}|}+\frac{1}{|\lambda_{c\beta i}|}\right)+O(\sqrt{\epsilon}) \qquad (25)$$

where x_{f0} and x_{s0} are the initial conditions for x_f and x_s in eq 19, respectively, and $\lambda_{c\alpha i}$ and $\lambda_{c\beta i}$ ($i = 1, 2, \cdots, m$) are the eigenvalues of Λ_{cs} in the system of eq 19.

Remark 6. Note that in order to regulate the surface roughness to a desired level, r_d, the number of actuators should be large enough so that the value of r_d is achievable.

Remark 7. Note that to control the expected value of the square of the surface roughness to $\langle r(\infty)^2\rangle$, we need to design a controller to assign the eigenvalues of the matrix Λ_{cs} in the system of eq 19 to appropriate values. The controller which assigns the eigenvalues of the matrix Λ_{cs} in the system of eq 19 to satisfy eq 25 is not unique. Consequently, for a fixed number of actuators, p, the controller that can drive the closed-loop surface roughness to a desired level is not unique either. Furthermore, we note that the proposed nonlinear feedback controller of eq 17 is a multivariable controller (i.e., the numbers of the manipulated inputs adjusted by this controller is equal to p). Therefore, the number of independent output variables that this controller is capable of simultaneously regulating is equal to p. If control of surface configuration variables other than the surface roughness is of interest (for example, surface coverage, island size, etc.), then these variables should be mathematically expressed as controlled outputs of the stochastic PDE and the nonlinear feedback controller should be designed to regulate these new outputs to the desired set-point values in a similar way to the one that is followed to achieve this task for the expected value of the surface roughness.

Remark 8. In case where the desired value of the steady-state surface roughness of the closed-loop system is r_d, the controller should be designed such that

$$r_d^{\,2} = \frac{1}{4\pi}\sum_{i=1}^{m}\left(\frac{1}{|\lambda_{c\alpha i}|}+\frac{1}{|\lambda_{c\beta i}|}\right)$$

Under this controller, the expected value of the square of surface roughness of the infinite-dimensional system is shown in eq 25, which is an $O(\sqrt{\epsilon})$ approximation of r_d^2, which means there exists a positive real number k_r such that $|\langle r(\infty)^2\rangle - r_d^2| < k_r \cdot \sqrt{\epsilon}$. Under the assumption that the number of control actuators is equal to the dimension of the x_s subsystem, the value of ϵ is dependent on the number of actuators used by the controller. Therefore, the larger the number of control actuators used, the smaller the ϵ. Consequently, the closed-loop surface roughness is closer to the desired surface roughness as the number of control actuators used to control the process increases. If the allowable error between the closed-loop surface roughness and the desired surface roughness is pre-specified as $e_r = |r_d^2 - \langle r(\infty)^2\rangle|$, then the number of control actuators should be chosen such that $k_r \cdot \sqrt{\epsilon} < e_r$ to achieve the desired closed-loop performance. However, it is not straightforward to solve for k_r analytically. Therefore, the number of control actuators can be determined using a two-step procedure. First, an estimate of the number of actuators, p_1 is made and an ϵ_1 is computed. Closed-loop simulations can be performed to evaluate the error between the expected closed-loop surface roughness and the desired value, $\bar{e}_{r1}$ when p_1 actuators are used. If $\bar{e}_{r1} > e_r$, then the number of actuators should be increased to p_2 (and the value of ϵ is reduced from ϵ_1 to ϵ_2) such that $\bar{e}_{r1} \cdot \sqrt{\epsilon_2} > e_r \cdot \sqrt{\epsilon_1}$ in order to achieve the desired closed-loop performance.

Remark 9. We note that a full-scale model of a sputtering process would consist of a two-dimensional (2D) lattice representation of the surface. Although we developed the method for nonlinear feedback control design based on a one-dimensional (1D) lattice representation of the surface, it is possible to extend the proposed method to control the surface roughness of material preparation processes taking place in 2D domains. In a 2D space process, the feedback control design and the analysis of the closed-loop system will be based on a two-dimensional extension of the model of eq 12. Moreover, eq 12 will be obtained by solving the eigenvalue/eigenfunction problem of the operator A in the 2D spatial domain subject to the appropriate boundary conditions; this can be achieved in a similar way to that followed for the 1D spatial domain (see recent work by Ni and Christofides[28] for results on the solution of the eigenvalue/eigenfunction problem for a 2D spatial domain). Once the modal representation of eq 12 corresponding to the 2D stochastic PDE is obtained, the method for control design and closed-loop analysis presented above can be applied to control the surface roughness.

4. Simulation Results

In this section, we present applications of the proposed nonlinear state feedback controller to the stochastic KSE to demonstrate that the nonlinear controller is able to regulate the expected value of the surface roughness to a desired level and to achieve an improved closed-loop performance over a linear controller. To demonstrate the applicability of the proposed control method to control surface directly formed by microscopic events, we also apply the nonlinear feedback controller to the kinetic Monte Carlo model of a sputtering process to demonstrate that the controller designed based on the stochastic KSE model of the process can drive the surface roughness in the kinetic Monte Carlo model of the same process to a desired level.

4.1. Nonlinear Control of the Stochastic KSE. In this subsection, we consider the following stochastic KSE with spatially distributed control:

$$\frac{\partial h}{\partial t} = -\nu\frac{\partial^2 h}{\partial x^2} - \kappa\frac{\partial^4 h}{\partial x^4} + \frac{\lambda}{2}\left(\frac{\partial h}{\partial x}\right)^2 + \sum_{i=1}^{p}\hat{b}_i(x)u_i(t) + \xi'(x,t) \qquad (26)$$

where u_i is the ith manipulated input, p is the number of manipulated inputs, $\hat{b}_i$ is the ith actuator distribution function (i.e., $\hat{b}_i$ determines how the control action computed by the ith control actuator, u_i, is distributed (e.g., point or distributed actuation) in the spatial interval $[-\pi, \pi]$), $\nu = 1.975 \times 10^{-4}$, $\kappa = 1.58 \times 10^{-4}$, $\lambda = 1.975 \times 10^{-4}$, $x \in [-\pi, \pi]$ is the spatial coordinate, t is the time, $h(x, t)$ is the height of the surface at position x and time t, and $\xi'(x, t)$ is a Gaussian noise with zero mean and covariance:

$$\langle \xi'(x,t)\xi'(x',t')\rangle = \varsigma^2\delta(x-x')\delta(t-t') \qquad (27)$$

where $\varsigma = 3.52 \times 10^{-5}$. Note that the difference between eq 1 and eq 26 is that in eq 26, the covariance of the Gaussian noise, $\xi'(x, t)$, is $\varsigma^2\delta(x - x')\delta(t - t')$ while in eq 1, the covariance of the Gaussian noise, $\xi(x, t)$, is $\delta(x - x')\delta(t - t')$.

We normalize the covariance of the Gaussian noise in the system of eq 26 to be $\delta(x - x')\delta(t - t')$ by introducing a new variable for the height of the surface, $h'(x, t) = h(x, t)/\varsigma$ and new actuator distribution functions, $b_i(x) = \hat{b}_i(x)/\varsigma$, for $i = 1, \cdots, p$. Equation 26, therefore, can be rewritten as follows:

$$\frac{\partial h'}{\partial t} = -\nu\frac{\partial^2 h'}{\partial x^2} - \kappa\frac{\partial^4 h'}{\partial x^4} + \frac{\lambda}{2}\left(\frac{\partial h'}{\partial x}\right)^2 + \sum_{i=1}^{p} b_i(x)u_i(t) + \xi(x, t) \quad (28)$$

where $\xi(x, t) = \xi'(x, t)/\varsigma$ and $\langle \xi(x, t)\xi(x', t')\rangle = \delta(x - x')\delta(t - t')$. Therefore, the system of eq 28 is consistent to the system of eq 1 which is the basis for feedback control design and closed-loop analysis. We also use the system of eq 28 for all simulations in this work.

A 200th order stochastic ordinary differential equation approximation of eq 28 obtained via Galerkin's method is used to simulate the process (the use of higher-order approximations led to identical numerical results, thereby implying that the following simulation runs are independent of the discretization). The δ function involved in the covariances of $\xi_\alpha{}^n$ and $\xi_\beta{}^n$ is approximated by $1/\Delta t$, where Δt is the integration time step.

4.1.1. Open-Loop Dynamics of the Stochastic KSE. In the first simulation, we compute the expected value of open-loop surface roughness profile from the solution of the stochastic KSE of eq 28 by setting $u_i(t) = 0$ for $i = 1, ..., p$. For $\nu = 1.975 \times 10^{-4}$ and $\kappa = 1.58 \times 10^{-4}$, the stochastic KSE possesses one positive eigenvalue. Therefore, the zero solution of the open-loop system is unstable. Surface roughness profiles obtained from 100 independent simulation runs using the same parameters are averaged and the resulting expected surface roughness profile is shown in Figure 1. The value of the open-loop surface roughness increases due to the open-loop instability of the zero solution.

4.1.2. Closed-Loop Simulation of the Stochastic KSE under Nonlinear Control. In the closed-loop simulation under nonlinear control, we design a nonlinear state feedback controller based on a 20th order stochastic ODE approximation constructed by using the first 20 eigenmodes of the system of eq 8 and apply this controller to a 200th order approximation of the nonlinear stochastic KSE. Twenty control actuators are used to control the system. The *i*th actuator distribution function is taken to be:

$$b_i(z) = \begin{cases} \frac{1}{\sqrt{\pi}}\sin(iz); & i = 1, ..., 10 \\ \frac{1}{\sqrt{\pi}}\cos[(i - 10)z]; & i = 11, ..., 20 \end{cases} \quad (29)$$

Under this control problem formulation, $m = 10$ and the value of $\epsilon = |\lambda_1|/|\lambda_{11}| = 1.73 \times 10^{-5}$. Our desired expected value of the surface roughness is 6.53.

Using eq 25, we design the nonlinear state-feedback controller such that $\lambda_{c\alpha_i} = \lambda_{c\beta_i} = -0.0373$, for $i = 1, ..., 10$. Closed-loop simulations are performed to study the evolution of the expected value of the surface roughness under nonlinear state feedback control. Closed-loop surface roughness profiles obtained from 100 independent simulation runs using the same simulation parameters are averaged, and the resulting closed-loop expected surface roughness profile is shown in Figure 2 (solid line) and compared with the open-loop expected surface roughness profile (dotted line). We can see that the controller successfully drives the surface roughness to the desired level, which is lower than that corresponding to open-loop operation ($u_i(t) = 0$, $i = 1, ...$, 20).

4.1.3. Comparison of Closed-Loop Performance under Nonlinear and Linear Control. In this subsection, we demonstrate that the performance of the proposed nonlinear controller is superior to the one of the linear state feedback controller resulting from the linearization of the nonlinear controller around the zero solution. The nonlinear controller is the same to that presented in section 4.1.2. The linear state feedback controller is designed based on a 20*th* order stochastic ODE approximation constructed by using the first 20 eigenmodes of the system of eq 8 as follows:

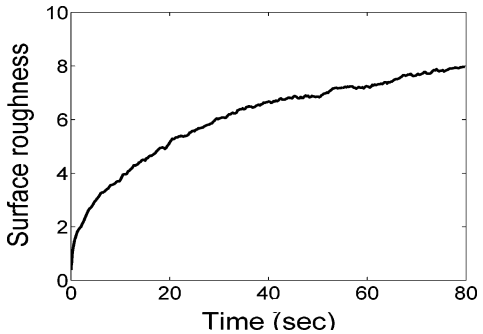

Figure 1. Open-loop profile of the expected surface roughness resulting from the computation of the average of 100 independent simulation runs of the stochastic KSE of eq 28.

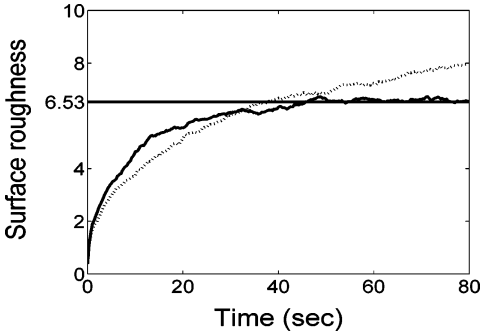

Figure 2. Closed-loop profile of the expected value of the surface roughness (solid line) vs open-loop profile of the expected value of the surface roughness (dotted line) when the controller is designed based on the first 20 modes.

$$u = B_s{}^{-1}(\Lambda_{cs} - \Lambda_s)\tilde{x}_s \quad (30)$$

where the definitions of the matrices B_s, Λ_{cs}, and Λ_s are the same as those in eq 17 and $\tilde{x}_s = [\alpha_1 \cdots \alpha_{10}\, \beta_1 \cdots \beta_{10}]^T$. Twenty control actuators are used to control the system. The *i*th actuator distribution function is the same to that shown in eq 29. The desired expected value of the surface roughness is 6.53, and the linear state feedback controller is designed such that $\lambda_{c\alpha_i} = \lambda_{c\beta_i} = -0.0373$, for $i = 1, ..., 10$. The linear controller is also applied to the 200th order approximation of the nonlinear stochastic KSE.

Closed-loop simulations are carried out to evaluate the performance of the closed-loop system achieved under the proposed nonlinear controller and to compare it to the one of the linear controller. Two cases are studied. In both cases, the desired expected surface roughness is 6.53, and the initial surface roughness is chosen to be 18 and 45, respectively. In each case, closed-loop simulation runs are carried out using both the linear state feedback controller (eq 30) and the nonlinear state feedback controller (eq 17). Further, in each case, the closed-loop surface roughness profiles are obtained by averaging 100 independent closed-loop simulation runs using the same simulation parameters and the resulting expected surface roughness profiles are presented in Figure 3. Moreover, in both cases, closed-loop surface roughness profiles under the linear and the nonlinear

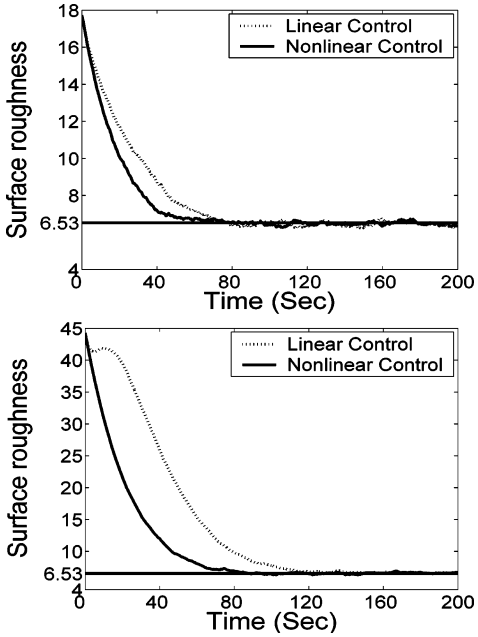

Figure 3. Comparison of the expected closed-loop surface roughness under the nonlinear controller (solid line) and that of the linear controller (dotted line) when the initial surface roughness is 18 (top) and 45 (bottom). The nonlinear controller performance is superior to the one of the linear controller.

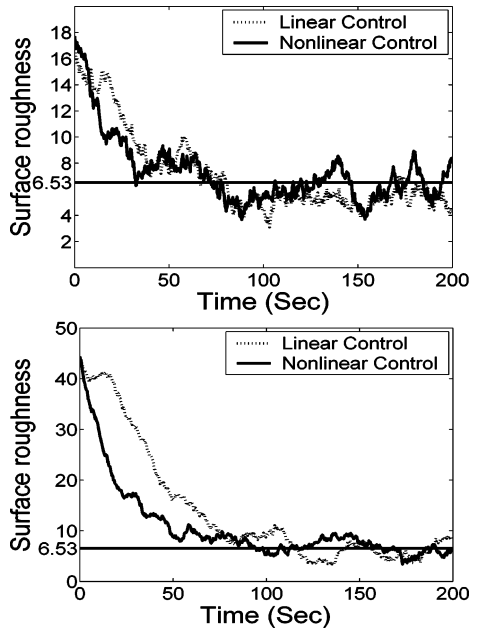

Figure 4. Comparison of the closed-loop surface roughness under the nonlinear controller (solid line) and that of the linear controller (dotted line) from a single simulation run when the initial surface roughness is 18 (top) and 45 (bottom). The nonlinear controller performance is superior to the one of the linear controller.

state feedback controllers obtained from a single simulation run using the same simulation parameters are presented in Figure 4.

The number of actuators used by both the linear controller and the nonlinear controller is the same (20 control actuators for all the closed-loop simulations discussed in this subsection). The parameters of the two controllers are the same except that the linear controller excludes the nonlinear term of the stochastic KSE. As a result, when the initial condition is small, both controllers are able to drive the expected closed-loop surface roughness to the desired level. However, based on the simulation results presented in Figure 3, it is clear that a large initial condition deteriorates the closed-loop performance under the linear controller while the nonlinear controller consistently achieves good closed-loop performance independently of the initial condition. This is because under the nonlinear feedback controller, the dominant modes of the closed-loop system of eq 19 (in particular, the first 20 modes) can be approximated by a stable linear stochastic system (see also eqs 41 and 51 in the Appendix). In a stable linear stochastic system, the decay rate of the expected value of the surface roughness to the set-point value depends on the eigenvalues of the matrix Λ_{cs} (assigned by the nonlinear controller) and is independent of the initial value of the state (see, for example, refs 26−28). Therefore, the closed-loop performance (in terms of rate of convergence of the expected value of surface roughness to the set-point) under the nonlinear controller is practically independent of the initial condition.

Remark 10. Note that a surface roughness profile obtained from one simulation run is one realization of a stochastic process. Due to the stochastic nature of the process, surface roughness profiles from different simulation runs using same simulation parameters are not identical, but will be around the expected surface roughness. Also, stochastic fluctuations can be observed in all simulation results. By averaging the surface roughness profiles from multiple independent simulation runs, the stochastic fluctuation can be reduced and the resulted profile is closer to the expected surface roughness. Conceptually, if we run a very large number of simulations with the same parameters, and average the roughness profiles obtained from each simulation run, the desired expected roughness profile can be obtained. In this study, we compute the expected values of surface roughness in both the open-loop and the closed-loop simulations by averaging surface roughness profiles obtained from 100 independent simulation runs. The resulted surface roughness profiles have little stochastic fluctuations and they are very close to the expected values. Furthermore, our control objective is to control the expected surface roughness to a desired level. In practice, a lower surface roughness is usually preferred. In our control problem formulation, if the expected surface roughness is controlled to a lower level compared to that in open-loop operation, it is expected that the surface roughness from each run will be lowered.

4.2. Application to a Sputtering Process Described by the Stochastic KSE. Physical processes whose evolution of surface height can be modeled by the stochastic KSE, such as surface erosion by ion sputtering, can also be modeled by using kinetic Monte Carlo techniques (see, for example, refs 7 and 26). Since kinetic Monte Carlo models predict the evolution of surface roughness in these processes by directly simulating the formation of the surface under various surface micro-processes such as adsorption, desorption, surface erosion and surface reaction, kinetic Monte Carlo models have a higher accuracy for prediction of the surface roughness than the stochastic KSE models do. To better verify the effectiveness of the developed feedback controller, we implement the proposed nonlinear feedback controller to the kinetic Monte Carlo process model of a sputtering process[7] to control the surface roughness to a desired level.

4.2.1. Process Description. We consider a 1D lattice representation of a crystalline surface in a sputtering process, which includes two surface microprocesses, erosion and diffusion. The solid-on-solid assumption is made which means that no defects or overhangs are allowed in the process.[41] The microscopic rules are as follows: a site, *i*, is first randomly

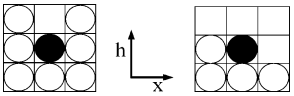

Figure 5. Schematic of the rule to determine P_e. P_e is defined as $^1/_7$ times the number of occupied sites in a box of size 3×3 centered at the particle on the top of site i; $P_e = 1$ in the left figure and $P_e = 4/7$ in the right figure, where the particle marked by ● is on the top of site i.

picked among the sites of the whole lattice and the particle at the top of this site is subject to (a) erosion with probability $0 < f < 1$ or (b) diffusion with probability $1 - f$.

If the particle at the top of site i is subject to erosion, the particle is removed from the site i with probability $P_e \cdot Y(\phi_i)$. P_e is determined as $^1/_7$ times the number of occupied sites in a box of size 3×3 centered at the site i, which is shown in Figure 5. There is a total of nine sites in the box. The central one is the particle to be considered for erosion (the one marked by ●). Among the remaining eight sites, the site above the central site of interest must be vacant since the central site is a surface site. Therefore, only seven of the eight sites can be occupied, and the maximum value of P_e is 1. $Y(\phi_i)$ is the sputtering yield function defined as follows:

$$Y(\phi_i) = y_0 + y_1\phi_i^2 + y_2\phi_i^4 \tag{31}$$

where y_0, y_1, and y_2 are process-dependent constants and ϕ_i is the local slope defined as follows:

$$\phi_i = \tan^{-1}\left(\frac{h_{i+1} - h_{i-1}}{2a}\right) \tag{32}$$

where a is the lattice parameter and h_{i+1} and h_{i-1} are the values of surface height at sites $i + 1$ and $i - 1$, respectively.

If the particle at the top of site i is subject to diffusion, one of its two nearest neighbors, j ($j = i + 1$ or $i - 1$) is randomly chosen, and the particle is moved to the nearest neighbor column with probability $w_{i\to j}$ as follows:

$$w_{i\to j} = \frac{1}{1 + \exp(\beta\Delta H_{i\to j})} \tag{33}$$

where $\Delta H_{i\to j}$ is the energy difference between the final and initial states of the move, $\beta = 1/k_BT$ and H is defined through the Hamiltonian of an unrestricted solid-on-solid model as follows:[41]

$$H = \left(\frac{J}{a^n}\right)\sum_{k=1}^{L}(h_k - h_{k+1})^n \tag{34}$$

where J is the bond energy, L is the total number of sites in the lattice, and n is a positive number. In the simulations presented in this paper, we use $n = 2$ and $\beta J = 2.0$.

The equation for the height fluctuations of the surface in this sputtering process was derived in ref 8 and is a stochastic KSE of the form of eq 35:

$$\frac{\partial h}{\partial t} = -\nu\frac{\partial^2 h}{\partial x^2} - \kappa\frac{\partial^4 h}{\partial x^4} + \frac{\lambda}{2}\left(\frac{\partial h}{\partial x}\right)^2 + \xi(x, t) \tag{35}$$

where $x \in [-\pi, \pi]$ is the spatial coordinate, t is the time, $h(x, t)$ is the height of the surface at position x and time t, ν and κ are two constants, and $\xi(x, t)$ is a Gaussian noise with zero mean and covariance:

$$\langle\xi(x, t)\xi(x', t')\rangle = \sigma^2\delta(x - x')\delta(t - t') \tag{36}$$

where σ is a constant, $\delta(\cdot)$ is the dirac function, and $\langle\cdot\rangle$ denotes the expected value. Note that the noise covariance depends on both space x and time t. We note that this stochastic KSE representation for the surface morphological evolution in sputtering processes is limited to surface morphologies that do not involve re-entrant features; the re-entrant features could arise under certain sputtering conditions and are catastrophic for the surface.

4.2.2. Open-Loop Dynamics of the Sputtering Process. In this section, we compute the expected surface roughness profile of the sputtering process by using both the kinetic Monte Carlo model and the stochastic KSE model of the process.

The following kinetic Monte Carlo simulation algorithm is used to simulate the sputtering process and to compute the surface roughness as well as the states $\alpha_n(t)$ and $\beta_n(t)$ of its corresponding stochastic KSE model:

The first random number, ζ_1 is generated to pick a site, i, among all the sites on the 1D lattice.

The second random number, ζ_2 in the (0, 1) interval, is generated to decide whether the chosen site, i, is subject to erosion ($\zeta_2 < \bar{f}$) or diffusion ($\zeta_2 > \bar{f}$).

If the chosen site is subject to erosion, P_e and $Y(\phi_i)$ are computed. P_e is computed by using the box rule shown in Figure 5 and the center of the box is the surface particle on site i and $Y(\phi_i)$ is computed by using eq 31 with $y_0 = 0.5$, $y_1 = 1.0065$, and $y_2 = -0.5065$. Then, another random number ζ_{e3} in the (0, 1) interval is generated. If $\zeta_{e3} < P_e \cdot Y(\phi_i)$, the surface particle on site i is removed. Otherwise, no Monte Carlo event is executed.

If the chosen site is subject to diffusion, a side neighbor, j, ($j = i + 1$ or $i - 1$ in the case of 1D lattice) is randomly picked and the hopping rate, $w_{i\to j}$, is computed by using eq 33. Then, another random number ζ_{d3} in the (0, 1) interval is generated. If $\zeta_{d3} < w_{ifj}$, the surface atom is moved to the new site. Otherwise no Monte Carlo event is executed.

Upon the execution of one Monte Carlo event, α_n or β_n are updated. If the executed event is erosion, α_n or β_n can be updated by using eq 37. If the executed event is diffusion from site i to site j, α_n or β_n are updated by using eq 38:

$$\alpha_n^{\text{new}} = \alpha_n^{\text{old}} + \frac{a[\psi(n, z_i - a/2) - \psi(n, z_i + a/2)]}{n}$$

$$\beta_n^{\text{new}} = \beta_n^{\text{old}} + \frac{a[\phi(n, z_i + a/2) - \phi(n, z_i - a/2)]}{n} \tag{37}$$

where a is the lattice parameter and z_i is the coordinates of the center of site i.

$$\alpha_n^{\text{new}} = \alpha_n^{\text{old}} + \frac{a\{[\psi(n, z_i - a/2) - \psi(n, z_i + a/2)] - [\psi(n, z_j - a/2) - \psi(n, z_j + a/2)]\}}{n}$$

$$\beta_n^{\text{new}} = \beta_n^{\text{old}} + \frac{a\{[\phi(n, z_i + a/2) - \phi(n, z_i - a/2)] - [\phi(n, z_j + a/2) - \phi(n, z_j - a/2)]\}}{n} \tag{38}$$

We also compute the expected surface roughness of the sputtering process based on its stochastic KSE process model of eq 35. A 200th order stochastic ordinary differential equation approximation of the system of eq 35 obtained via Galerkin's method is used to simulate the process (the use of higher-order approximations led to identical numerical results, thereby implying that the following simulation runs are independent of

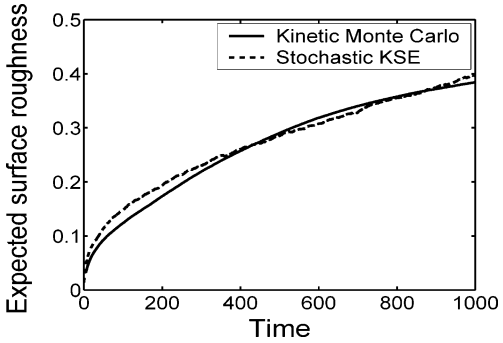

Figure 6. Comparison of the open-loop profile of the expected surface roughness from the kinetic Monte Carlo simulator (solid line) and that from the solution of the stochastic KSE process model (dotted line).

the discretization). The δ function involved in the covariances of $\xi_\alpha{}^n$ and $\xi_\beta{}^n$ is approximated by $1/\Delta t$ where Δt is the integration time step. The parameters of the stochastic KSE model are $\nu = 3.27 \times 10^{-6}$, $\kappa = 1.34 \times 10^{-8}$, $\lambda = 7.52 \times 10^{-6}$, and $\sigma = 4.65 \times 10^{-3}$.

In Figure 6, we compare the expected value of the open-loop surface roughness of the sputtering process from the solution of the stochastic KSE model of eq 35 to that from a kinetic Monte Carlo simulation. The two profiles are very close. Therefore, by using the stochastic KSE model of eq 35, we can predict the evolution of the expected surface roughness in this sputtering process. This stochastic KSE model is used as the basis for feedback controller design.

4.2.3. Feedback Control Design. Our control objective is to control the expected surface roughness in the sputtering process to a desired value. Based on the stochastic KSE model of the sputtering process (eq 35), a distributed control problem is formulated by following eq 26. We design a state feedback controller based on a 40th order stochastic ODE approximation constructed by using the first 40 eigenmodes of the stochastic KSE model of eq 35. Forty control actuators are used to control the system. The ith actuator distribution function is taken to be:

$$b_i(z) = \begin{cases} \frac{1}{\sqrt{\pi}}\sin(iz); & i = 1, ..., 20 \\ \frac{1}{\sqrt{\pi}}\cos[(i-20)z]; & i = 21, ..., 40 \end{cases} \tag{39}$$

The desired closed-loop surface roughness is 0.3 in this simulation. We design the state feedback controller such that $\lambda_{c\alpha_i} = \lambda_{c\beta_i} = -0.01$, for $i = 1, ,,,, 20$.

Then, we apply the designed controller to the kinetic Monte Carlo model of the sputtering process to control the surface roughness to the desired level. In this simulation, the initial surface roughness is about 0.5, and the microstructure of the initial surface is shown in Figure 7. The controller is implemented by manipulating the probability that a randomly selected site is subject to erosion rule, f. Specifically, the f of site i is determined according to the following expression:

$$f(i) = \frac{\bar{f} + (\sum_{j=1}^{40} b_j(z_i)u_j(t))/a}{1 + (\sum_{j=1}^{40} b_j(z_i)u_j(t))/a} \tag{40}$$

The following simulation algorithm is used to run the kinetic Monte Carlo simulations for the closed-loop system. First, a random number, ζ_1 is generated to pick a site i, among all the sites on the 1D lattice; the probability that a surface site is subject to the erosion rules, $f(i)$ is determined by using eq 40. Then, the second random number, ζ_2 in the (0, 1) interval is generated. If $\zeta_2 < f(i)$, the site i is subject to the erosion, otherwise, the site is subject to diffusion.

If the site i is subject to erosion, P_e is computed by using the box rule shown in Figure 5 with the box centering the surface particle on site i and $Y(\phi_i)$ is computed by using eq 31. Then, another random number, ζ_{e3} in the (0, 1) interval is generated. If $\zeta_{e3} < P_e \cdot Y(\phi_i)$ the surface particle on site i is removed. Otherwise, no Monte Carlo event is executed.

If the site i is subject to diffusion, a side-neighbor, $j = i + 1$ or $i - 1$ is randomly picked and the probability of a hopping from site i to site j, $w_{i\to j}$ is computed based on eq 33. Then, another random number ζ_{d3} in the (0, 1) interval is generated. If $\zeta_{e3} < w_{i\to j}$, the surface particle on site i is moved to site j. Otherwise, no Monte Carlo event is executed. Once a Monte Carlo event is executed, the first 40 states (α_1, ..., α_{20} and β_1, ..., β_{20}) are updated and new control actions are computed to update the value of f (defined in eq 40) for each surface site.

The closed-loop system simulation result is shown in Figure 8. The expected surface roughness, which is the average of surface roughness profiles obtained from 100 independent runs, under feedback control is plotted in solid line. We can see that the controller successfully drives the expected surface roughness to the desired value. The dotted line shows the surface roughness profile under feedback control from one simulation run; due to the stochastic nature of the sputtering process, stochastic fluctuations can be observed in the closed-loop surface roughness profile, but the surface roughness is very close to the expected surface roughness under the nonlinear feedback

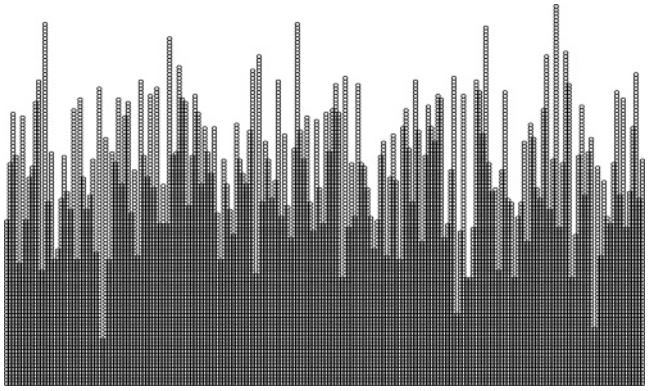

Figure 7. Surface microconfiguration at the beginning of the closed-loop simulation run.

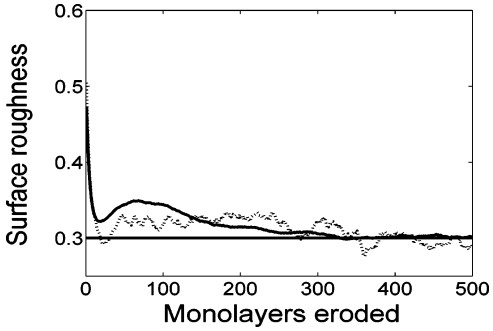

Figure 8. Closed-loop surface roughness profiles in the sputtering process. (a) The expected closed-loop surface roughness profile obtained from 100 independent simulation runs (solid line). (b) The closed-loop surface roughness profile from one simulation run (dotted line).

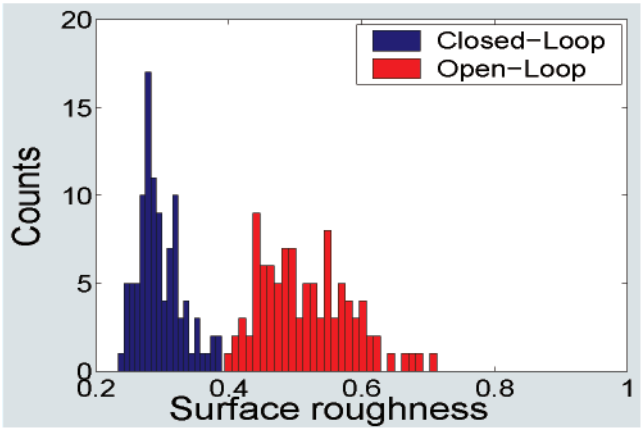

Figure 9. Histogram of final surface roughness of 100 closed-loop and 100 open-loop simulation runs.

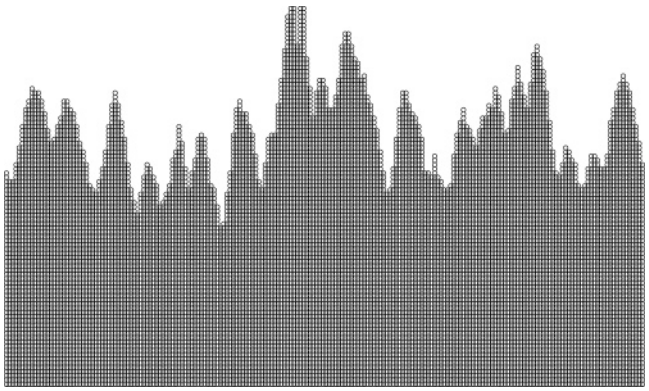

Figure 10. Surface microconfiguration at the end of the closed-loop simulation run under nonlinear feedback control.

control. We can see that under feedback control, the surface roughness can be controlled to the desired level.

Figure 9 shows the final surface roughness histogram after 500 monolayers are eroded using 100 different closed-loop simulation runs and that using 100 different open-loop simulation runs. It is clear that the surface roughness from closed-loop simulation runs is lower than that from open-loop simulation runs. Moreover, the variance of the final surface roughness from 100 closed-loop simulation runs is 0.067% while the variance of the final surface roughness from 100 open-loop simulation runs is 0.53%. The relative larger variance among the final surface roughness by open-loop simulations can be attributed to the stochastic nature of the sputtering process itself. As demonstrated in Figure 9, feedback control can not only reduce the expected final surface roughness, but also effectively reduce the variance of the final surface roughness.

The microstructure of the surface at the end of the closed-loop system simulation run is shown in Figure 10. It is clear that the proposed nonlinear feedback control method can reduce the surface roughness to the desired level.

5. Conclusions

In this work, we developed a method for nonlinear feedback control of the roughness of a one-dimensional surface whose evolution is described by the stochastic KSE. Our method includes the construction of a nonlinear feedback controller that can be readily implemented in practice and an analysis of the closed-loop infinite-dimensional system to characterize the closed-loop performance enforced by the nonlinear feedback controller. The effectiveness of the proposed nonlinear controller and the advantages of the nonlinear controller over a linear controller resulting from the linearization of the nonlinear controller around the zero solution were demonstrated through numerical simulations. Finally, a successful application of a stochastic KSE-based nonlinear feedback controller to the kinetic Monte Carlo model of a sputtering process was also demonstrated.

Acknowledgment

Financial support from the NSF (CTS-0325246) is gratefully acknowledged by P.D.C.

Appendix

Proof of Theorem 1. The proof of Theorem 1 includes three parts. First, we compute the contribution to the expected surface roughness from the x_f subsystem of eq 19 and prove eq 23 in Theorem 1. Then, we compute the contribution to the expected surface roughness from the x_s subsystem of eq 19 and prove eq 24 in Theorem 1. Finally, the proof of Theorem 1 is completed by proving eq 25 based on the results in eqs 23 and 24. Since we work with sufficiently small initial conditions, local stability of the closed-loop nonlinear infinite-dimensional system can be proved by using the linearization argument of section 3.3 and is used without further proof in the remainder.

Proof of Equation 23 in Theorem 1. Consider the closed-loop system of eq 19 and note that the terms in the right-hand-side of the x_f subsystem constitute an $O(\epsilon)$ approximation to the term $\Lambda_{f\epsilon}x_f$. Consider also the following linear system:

$$\epsilon\frac{d\bar{x}_f}{dt} = \Lambda_{f\epsilon}\bar{x}_f + \epsilon\xi_f \tag{41}$$

Following a similar approach to the one employed in the proof of Theorem A.1 in ref 42, p 361, we have that there exists an $\hat{\epsilon}^* > 0$ such that for all $\epsilon \in (0, \hat{\epsilon}^*]$, we have

$$x_f(t) = \bar{x}_f(t) + O(\sqrt{\epsilon}) \tag{42}$$

Therefore, we have the following estimate for $\langle||x_f(t)||_2^2\rangle$:

$$\langle||x_f(t)||_2^2\rangle = \langle||\bar{x}_f(t) + O(\sqrt{\epsilon})||_2^2\rangle \leq 2\langle||\,\bar{x}_f(t)||_2^2\rangle + O(\epsilon) \tag{43}$$

Furthermore, $\langle||x_f(t)||_2^2\rangle$ and $\langle||\bar{x}_f(t)||_2^2\rangle$ are equal to the traces of the covariance matrices of $x_f(t)$ and $\bar{x}_f(t)$, $P_f(t) = \langle x_f(t)x_f(t)^T\rangle$, and $\bar{P}_f(t) = \langle\bar{x}_f(t)\bar{x}_f(t)^T\rangle$, respectively. Finally, as $t \to \infty$, $P_f(t)$ and $\bar{P}_f(t)$ converge to $P_f(\infty)$ and $\bar{P}_f(\infty)$, respectively (both $P_f(\infty)$ and $\bar{P}_f(\infty)$ are bounded quantities which follows from closed-loop stability). We note that the 2-norm of x_f, $||x_f||_2$, is defined in eq 14 and $P_f(\infty)$ is defined in eq 21. Because $\Lambda_{f\epsilon}$ is a diagonal matrix, the trace of matrix $\bar{P}_f$ can be computed as follows:[26]

$$\mathrm{Tr}\{\bar{P}_f\} = \frac{\epsilon}{2}\cdot\sum_{i=1}^{\infty}\left|\frac{1}{\lambda_{\epsilon i}}\right| \tag{44}$$

where $\lambda_{\epsilon i}$ ($i = 1, 2, ..., \infty$) are the eigenvalues of the matrix $\Lambda_{f\epsilon}$ in eq 41. Specifically, $|\lambda_{\epsilon 1}| = |\nu - \kappa|$ and $|\lambda_{\epsilon i}| = |(\nu - \kappa)[\nu(2m + i)^2 - \kappa(2m + i)^4]/[\nu(2m + 1)^2 - \kappa(2m + 1)^4]|$ ($i = 1, 2, ..., \infty$). It is clear that $|\lambda_{\epsilon i}|$ increases with respect to i in the order of $(2m + i)$,[4] where $2m$ is the size of the x_s subsystem in eq 19. Therefore, $\Sigma_{i=1}^{\infty}|1/\lambda_{\epsilon i}|$ converges to a finite positive number. Thus, there exists a positive real number $k_{f\epsilon}$ such that

$$\mathrm{Tr}\{\bar{P}_f\} < \frac{\epsilon}{2} \cdot k_{f\epsilon} \tag{45}$$

Therefore, it follows that

$$\mathrm{Tr}\{\bar{P}_f\} = \langle || \bar{x}_f(\infty)||_2^2 \rangle = O(\epsilon) \tag{46}$$

According to eq 43, it follows that the contribution to the expected surface roughness from x_f is $O(\epsilon)$, i.e.:

$$\langle r_f(\infty)^2 \rangle = \frac{1}{2\pi}\langle ||x_f(\infty)||_2^2 \rangle = \frac{1}{2\pi}\sum_{i=m+1}^{\infty} [\langle \alpha_i(\infty)^2 \rangle + \langle \beta_i(\infty)^2 \rangle] = O(\epsilon) \tag{47}$$

This completes the proof of eq 23 in Theorem 1.

Proof of Equation 24 in Theorem 1. Consider the x_s subsystem of the closed-loop system of eq 19. First, we note that there exists a positive real number k_{1s} such that[39,43]

$$||f_s(x_s, x_f) - f_s(x_s, 0)||_2 < k_{1s}||x_f||_2 \tag{48}$$

where the definitions of $||x_f||_2$ and $||f_s(\cdot)||_2$ can be found in eq 14. From eq 42, we have the following estimate for $||x_f||_2$ for $t \geq t_b$ (where t_b is the time needed for $|| \bar{x}_f(t)||$ to approach zero and $t_b \to 0$ as $\epsilon \to 0$):

$$||x_f(t)||_2 = \sqrt{\sum_{i=m+1}^{\infty} [\langle \alpha_i(\infty)^2 \rangle + \langle \beta_i(\infty)^2 \rangle]} = O(\sqrt{\epsilon}) \tag{49}$$

This implies that we have the following estimate for $||f_s(x_s, x_f) - f_s(x_s, 0)||_2$ for $t \geq t_b$:

$$||f_s(x_s, x_f) - f_s(x_s, 0)||_2 = O(\sqrt{\epsilon}) \tag{50}$$

Therefore, the solution of the following system consists an $O(\sqrt{\epsilon})$ approximation of the x_s of eq 19 [ref 42, Theorem A.1, p 361]:

$$\frac{d\bar{x}_s}{dt} = \Lambda_{cs}\bar{x}_s + \xi_s \tag{51}$$

In particular, there exists an $\hat{\epsilon}^{**} > 0$ such that for all $\epsilon \in (0, \hat{\epsilon}^{**}]$, it holds that

$$x_s(t) - \bar{x}_s(t) = O(\sqrt{\epsilon}) \tag{52}$$

and

$$||x_s(t)||_2^2 - || \bar{x}_s(t)||_2^2 = (||x_s(t)||_2 - || \bar{x}_s(t)||_2) \cdot (||x_s(t)||_2 + || \bar{x}_s(t)||_2) = O(\sqrt{\epsilon}) \tag{53}$$

Because $||x_s(t)||_2$ and $||\bar{x}_s(t)||_2$ are bounded for all $t > 0$, $\langle ||x_s(t)||_2^2 \rangle$ and $\langle ||\bar{x}_s(t)||_2^2 \rangle$ are equal to the traces of the covariance matrices of $x_s(t)$ and $\bar{x}_s(t)$, $P_s(t) = \langle x_s(t)x_s(t)^T \rangle$ and $\bar{P}_s(t) = \langle \bar{x}_s(t)\bar{x}_s(t)^T \rangle$, respectively. As $t \to \infty$, $P_s(t)$ and $\bar{P}_s(t)$ converge to $P_s(\infty)$ and $\bar{P}_s(\infty)$, respectively. The definition of $P_s(\infty)$ can be found in eq 21.

Because Λ_{cs} is a diagonal matrix, the trace of matrix $\bar{P}_s(\infty)$ can be computed as follows:[26]

$$\mathrm{Tr}\{\bar{P}_s(\infty)\} = \frac{1}{2}\sum_{i=1}^{m}\left(\left|\frac{1}{\lambda_{c\alpha i}}\right| + \left|\frac{1}{\lambda_{c\beta i}}\right|\right) \tag{54}$$

where $\lambda_{c\alpha i}$ and $\lambda_{c\beta i}$ ($i = 1, 2, ..., m$) are the eigenvalues of the matrix Λ_{cs} in eq 19. Therefore, it holds that

$$\langle ||\bar{x}_s(\infty)||_2^2 \rangle = \mathrm{Tr}\{\bar{P}_s(\infty)\} = \frac{1}{2}\sum_{i=1}^{m}\left(\left|\frac{1}{\lambda_{c\alpha i}}\right| + \left|\frac{1}{\lambda_{c\beta i}}\right|\right) \tag{55}$$

According to eq 53, it holds that the contribution to the expected surface roughness from x_s is as follows:

$$\langle r_s(\infty)^2 \rangle = \frac{1}{2\pi}\langle ||x_s(\infty)||_2^2 \rangle = \frac{1}{2\pi}\sum_{i=1}^{m} [\langle \alpha_i(\infty)^2 \rangle + \langle \beta_i(\infty)^2 \rangle] = \frac{1}{4\pi}\sum_{i=1}^{m}\left(\left|\frac{1}{\lambda_{c\alpha i}}\right| + \left|\frac{1}{\lambda_{c\beta i}}\right|\right) + O(\sqrt{\epsilon}) \tag{56}$$

This completes the proof of eq 24 in Theorem 1.

Proof of Equation 25 in Theorem 1. The expected surface roughness from the closed-loop system, $\langle r(\infty)^2 \rangle$, includes contributions from both the x_s subsystem and the x_f subsystem of eq 19. Therefore, we have the following equation for $\langle r(\infty)^2 \rangle$:

$$\langle r(\infty)^2 \rangle = \langle r_s(\infty)^2 \rangle + \langle r_f(\infty)^2 \rangle \tag{57}$$

Using eqs 23 and 24, we immediately have

$$\langle r(\infty)^2 \rangle = \frac{1}{4\pi}\sum_{i=1}^{m}\left(\frac{1}{|\lambda_{c\alpha i}|} + \frac{1}{|\lambda_{c\beta i}|}\right) + O(\sqrt{\epsilon}) + O(\epsilon) \tag{58}$$

Since as $\epsilon \to 0$, it holds that

$$\frac{O(\epsilon)}{O(\sqrt{\epsilon})} \to 0 \tag{59}$$

The $O(\epsilon)$ term in eq 58 is negligible, and there exists an $\epsilon^* = \min(\hat{\epsilon}^*, \hat{\epsilon}^{**})$ such that if $\epsilon \in (0, \epsilon^*]$, then

$$\langle r(\infty)^2 \rangle = \frac{1}{4\pi}\sum_{i=1}^{m}\left(\frac{1}{|\lambda_{c\alpha i}|} + \frac{1}{|\lambda_{c\beta i}|}\right) + O(\sqrt{\epsilon}) \tag{60}$$

where $\lambda_{c\alpha i}$, $\lambda_{c\beta i}$ ($i = 1, 2, ..., m$) are eigenvalues of Λ_{cs} in the system of eq 19. This completes the proof of Theorem 1.

Literature Cited

(1) Gillespie, D. T. A general method for numerically simulating the stochastic time evolution of coupled chemical reactions. *J. Comput. Phys.* **1976**, *22*, 403−434.

(2) Fichthorn, K. A.; Weinberg, W. H. Theoretical foundations of dynamical Monte Carlo simulations. *J. Chem. Phys.* **1991**, *95*, 1090−1096.

(3) Shitara, T.; Vvedensky, D. D.; Wilby, M. R.; Zhang, J.; Neave, J. H.; Joyce, B. A. Step-density variations and reflection high-energy electron-diffraction intensity oscillations during epitaxial growth on vicinal GaAs-(001). *Phys. Rev. B* **1992**, *46*, 6815−6824.

(4) Reese, J. S.; Raimondeau, S.; Vlachos, D. G. Monte Carlo algorithms for complex surface reaction mechanisms: efficiency and accuracy. *J. Comput. Phys.* **2001**, *173*, 302−321.

(5) Edwards, S. F.; Wilkinson, D. R. The surface statistics of a granular aggregate. *Proc. R. Soc. London A* **1982**, *381*, 17−31.

(6) Vvedensky, D. D.; Zangwill, A.; Luse, C. N.; Wilby, M. R. Stochastic equations of motion for epitaxial growth. *Phys. Rev. E* **1993**, *48*, 852−862.

(7) Cuerno, R.; Makse, H. A.; Tomassone, S.; Harrington, S. T.; Stanley, H. E. Stochastic model for surface erosion via ion sputtering: dynamical evolution from ripple morphology to rough morphology. *Phys. Rev. Lett.* **1995**, *75*, 4464−4467.

(8) Lauritsen, K. B.; Cuerno, R.; Makse, H. A. Noisy Kuramote−Sivashinsky equation for an erosion model. *Phys. Rev. E* **1996**, *54*, 3577−3580.

(9) Zapien, J. A.; Messier, R.; Collin, R. W. Ultraviolet-extended real-time spectroscopic ellipsometry for characterization of phase evolution in BN thin films. *Appl. Phys. Lett.* **2001**, *78*, 1982−1984.

(10) Renaud, G.; Lazzari, R.; Revenant, C.; Barbier, A.; Noblet, M.; Ulrich, O.; Leroy, F.; Jupille, J.; Borensztein, Y.; Henry, C. R.; Deville, J. P.; Scheurer, F.; Mane-Mane, J.; Fruchart, O. Real-time monitoring of growing nanoparticles. *Science* **2003**, *300*, 1416−1419.

(11) Ni, D.; Lou, Y.; Christofides, P. D.; Sha, L.; Lao, S.; Chang, J. P. Real-time carbon content control for PECVD ZrO_2 thin-film growth. *IEEE Trans. Semicond. Manuf.* **2004**, *17*, 221−230.

(12) Voigtländer, B. Fundamental processes in Si/Si and Ge/Si studied by scanning tunneling microscopy during growth. *Surf. Sci. Rep.* **2001**, *43*, 127−254.

(13) Lou, Y.; Christofides, P. D. Estimation and control of surface roughness in thin film growth using kinetic Monte Carlo models. *Chem. Eng. Sci.* **2003**, *58*, 3115−3129.

(14) Lou, Y.; Christofides, P. D. Feedback control of growth rate and surface roughness in thin film growth. *AIChE J.* **2003**, *49*, 2099−2113.

(15) Lou, Y.; Christofides, P. D. Feedback control of surface roughness of GaAs (001) thin films using kinetic Monte Carlo models. *Comput. Chem. Eng.* **2004**, *29*, 225−241.

(16) Ni, D.; Christofides, P. D. Dynamics and control of thin film surface microstructure in a complex deposition process. *Chem. Eng. Sci.* **2005**, *60*, 1603−1617.

(17) Siettos, C. I.; Armaou, A.; Makeev, A. G.; Kevrekidis, I. G. Microscopic/stochastic timesteppers and "coarse" control: a kMC example. *AIChE J.* **2003**, *49*, 1922−1926.

(18) Armaou, A.; Siettos, C. I.; Kevrekidis, I. G. Time-steppers and 'coarse' control of distributed microscopic processes. *Int. J. Robust Nonlinear Control* **2004**, *14*, 89−111.

(19) Kardar, M.; Parisi, G.; Zhang, Y. C. Dynamic scaling of growing interfaces. *Phys. Rev. Lett.* **1986**, *56*, 889−892.

(20) Ballestad, A.; Ruck, B. J.; Schmid, J. H.; Adamcyk, M.; Nodwell, E.; Nicoll, C.; Tiedje, T. Surface morphology of GaAs during molecular beam epitaxy growth: comparison of experimental data with simulations based on continuum growth equations. *Phys. Rev. B* **2002**, *65*, 205302.

(21) Kan, H. C.; Shah, S.; Tadyyon-Eslami, T.; Phaneuf, R. J. Transient evolution of surface roughness on patterned GaAs(001) during homoepitaxial growth. *Phys. Rev. Lett.* **2004**, *92*, 146101.

(22) Gallivan, M. A.; Murray, R. M. Reduction and identification methods for markovian control systems, with application to thin film deposition. *Int. J. Robust Nonlinear Control* **2004**, *14*, 113−132.

(23) Rusli, E.; Drews, T. O.; Ma, D. L.; Alkire, R. C.; Braatz, R. D. Robust nonlinear feedforward-feedback control of a coupled kinetic monte carlo-finite difference simulation. *J. Process Control* **2006**, *16*, 409−417.

(24) Villain, J. Continuum models of crystal growth from atomic beams with and without desorption. *J. Phys. I* **1991**, *1*, 19−42.

(25) Lou, Y.; Christofides, P. D. Feedback control of surface roughness using stochastic PDEs. *AIChE J.* **2005**, *51*, 345−352.

(26) Lou, Y.; Christofides, P. D. Feedback control of surface roughness in sputtering processes using the stochastic Kuramoto−Sivashinsky equation. *Comput. Chem. Eng.* **2005**, *29*, 741−759.

(27) Ni, D.; Christofides, P. D. Construction of stochastic PDEs for feedback control of surface roughness in thin film deposition. In *Proceedings of American Control Conference*, Portland, OR; 2005; pp 2540−2547.

(28) Ni, D.; Christofides, P. D. Multivariable predictive control of thin film deposition using a stochastic PDE model. *Ind. Eng. Chem. Res.* **2005**, *44*, 2416−2427.

(29) Insepov, Z.; Yamada, I.; Sosnowski, M. Surface smoothing with energetic cluster beams. *J. Vac. Sci. Technol. A* **1997**, *15*, 981−984.

(30) Qi, H. J.; Huang, L. H.; Tang, Z. S.; Cheng, C. F.; Shao, J. D.; Fan, Z. X. Roughness evolution of ZrO_2 thin films grown by reactive ion beam sputtering. *Thin Solid Films* **2003**, *444*, 146−152.

(31) Armaou, A.; Christofides, P. D. Wave suppression by nonlinear finite-dimensional control. *Chem. Eng. Sci.* **2000**, *55*, 2627−2640.

(32) Armaou, A.; Christofides, P. D. Feedback control of the Kuramoto-Sivashinsky equation. *Physica D* **2000**, *137*, 49−61.

(33) Christofides, P. D.; Armaou, A. Global stabilization of the Kuramoto−Sivashinsky equation via distributed output feedback control. *Syst. Control Lett.* **2000**, *39*, 283−294.

(34) Lou, Y.; Christofides, P. D. Optimal actuator/sensor placement for nonlinear control of the Kuramoto−Sivashinsky equation. *IEEE Trans. Control Syst. Technol.* **2003**, *11*, 737−745.

(35) Åström, K. J. *Introduction to Stochastic Control Theory*; Academic Press: New York, 1970.

(36) Choo, J. O.; Adomaitis, R. A.; Henn-Lecordier, L.; Cai, Y.; Rubloff, G. W. Development of a spatially controllable chemical vapor deposition reactor with combinatorial processing capabilities. *Rev. Sci. Instrum.* **2005**, *76*, 062217.

(37) Vvedensky, D. D. Edwards−Wilkinson equation from lattice transition rules. *Phys. Rev. E* **2003**, *67*, 025102(R).

(38) Temam, R. *Infinite-Dimensional Dynamical Systems in Mechanics and Physics*; Springer-Verlag: New York, 1988.

(39) Christofides, P. D.; Daoutidis, P. Finite-dimensional control of parabolic PDE systems using approximate inertial manifolds. *J. Math. Anal. Appl.* **1997**, *216*, 398−420.

(40) Liu, W. J.; Krstić, M. Stability enhancement by boundary control in the Kuramoto−Sivashinsky equation. *Nonlinear Anal.: Theory, Methods Appl.* **2001**, *43*, 485−507.

(41) Siegert, M.; Plischke, M. Solid-on-solid models of molecular-beam epitaxy. *Phys. Rev. E* **1994**, *50*, 917−931.

(42) Kokotovic, P. V.; Khalil, H. K.; O'Reilly, J. *Singular Perturbations in Control*: *Analysis and Design*; Academic Press: London, 1986.

(43) Christofides, P. D. *Nonlinear and Robust Control of PDE Systems*: *Methods and Applications to Transport-Reaction Processes*; Birkhäuser: Boston, 2001.

Received for review March 31, 2006
Revised manuscript received May 23, 2006
Accepted August 1, 2006

IE060410H